

# Critical currents in Josephson junctions, with unconventional pairing symmetry:

$$d_{x^2-y^2} + is \text{ versus } d_{x^2-y^2} + id_{xy}$$

N. Stefanakis, N. Flytzanis

Department of Physics, University of Crete, P.O. Box 2208, GR-71003, Heraklion, Crete, Greece

(December 2, 2024)

The critical currents and the spontaneous flux in unconventional Josephson junctions of superconductors with time reversal broken symmetry  $T$  and parity  $P$  are calculated as a function of the grain orientation. Two possible states are examined i.e.  $d_{x^2-y^2} + is$ ,  $d_{x^2-y^2} + id_{xy}$ , both violate the  $T$ , and parity  $P$ . We study the stability of the spontaneously formed fractional vortex and antivortex. An experiment based on the Josephson effect is proposed, which may provide a way to distinguish between these two symmetries.

## I. INTRODUCTION

One of the main questions in the research activity on high- $T_c$  superconductors nowadays is the identification of the order parameter symmetry [1,2]. The most possible scenario is that the pairing state has a  $d_{x^2-y^2}$ -wave character. Theoretical calculations, suggest that a two component order parameter is realized in a certain temperature range or under some perturbation. The observation of fractional vortices on the grain boundary in  $\text{YBa}_2\text{Cu}_3\text{O}_7$  by Kirtley *et al.* [3], may indicate a possible violation of the time-reversal symmetry near grain boundary. Patches of complex  $d_{xy}$  components are induced around magnetic impurities at low temperatures in a  $d_{x^2-y^2}$ -wave superconductor forming a phase coherent state as a result of tunneling between different patches [4]. Violation of parity and time reversal symmetry occurs in this state. Also on the high field region,  $H \leq H_{c2}$  the  $d_{x^2-y^2}$ -wave state can be perturbed by the external field, producing a  $d_{x^2-y^2} + id_{xy}$  state in the bulk [5]. The observation of the splitting of the zero energy peak in the conductance spectra at low temperatures indicates that a secondary component is induced which violates locally the time reversal symmetry [6]. Theoretical explanation based on surface-induced Andreev states, has been proposed [7]. Recently the field dependence of this splitting has been observed in the tunneling spectra of YBCO [8,9]. This observation is consistent with a  $d_{x^2-y^2} + is$  surface order parameter or a  $d_{x^2-y^2} + id_{xy}$  bulk order parameter.

In this work we present a definite qualitative argument based on the Josephson effect, which may be used to clarify this point. We study the static properties of a frustrated junction which is made of two one-dimensional junctions, with  $d_{x^2-y^2} + is$  or  $d_{x^2-y^2} + id_{xy}$  symmetry. By introducing an extra relative phase in each part of this junction, the above junction can be mapped into the corner junctions experiments [2,10]. The magnetic inter-

ference patterns of such a junction has been presented in a previous work [11]. The critical current  $I_c$  that a junction can carry versus the grain orientation is calculated by solving numerically the sine-Gordon equation. The magnetic flux of fractional vortices, or antivortices which are spontaneously formed as a consequence of the symmetry, is calculated for the different states we propose.

The physical meaning of the vortex, antivortex solutions is discussed in Ref. [12], where they study using the s-G equation the vortex-antivortex pair that exist at both ends of a  $0 - \pi - 0$  junction theoretically. Also the existence of stable solutions with flux  $\Phi = \pm\Phi_0/2$  has been examined by Bailey et. al. in Ref. [13] where they study a triangular grain boundary in  $d$ -wave superconductors. They conclude that under the assumption of  $d$ -wave symmetry the flux at the edges of this triangle can take the values  $\pm\Phi_0/2$ . Of course due to the periodic boundary conditions, on the phase  $\phi$ , the total flux integrated over the whole triangle interface is integer multiple of  $\Phi_0$ . However in the case of  $d_{x^2-y^2} + is$  symmetry they considered that an intrinsic phase shift  $\phi_c(x)$  exists in each triangle edge. They stated that the phase  $\phi(x)$  must change in order to connect the different values of  $\phi_c$  in each segment. This arrangement leads to fractional vortices or antivortices at each three corners.

The rest of the paper is organized as follows. In Sec. II we discuss the Josephson effect between two superconductors with mixed wave symmetry. In Sec. III the geometry of the junction is discussed. In Sec. IV we present the results for the magnetic flux and the critical current. In Sec. V the magnetic field effect is considered. Finally, a summary and discussion are presented in the last section.

## II. JOSEPHSON EFFECT BETWEEN TWO SUPERCONDUCTORS WITH MIXED WAVE SYMMETRY

We consider the junction shown in Fig. 1(a), where two superconductors ( $A$  in the region  $z > t$  and  $B$  in the region  $z < 0$ ), are separated by an intermediate layer. We assume that each superconductor has a two component order parameter. The order parameter for each component  $k$  ( $k = 1, 2$ ) in the superconductors, can be written as

$$n_k = \begin{cases} \tilde{n}_k^A e^{i\phi_k^A}, & z > t \\ \tilde{n}_k^B e^{i\phi_k^B}, & z < 0 \end{cases}, \quad (1)$$

Here  $\phi_k^{A(B)}$  is the phase of the order parameter  $n_k$  in superconductor  $A(B)$ .

The approximation of small barrier thickness compared to the coherence length [14], leads to a linear variation of the order parameter across the interface from the one edge with phase  $\phi_k^A$  to the other with phase  $\phi_k^B$ . Then the supercurrent density can be written as [15]

$$J = \sum_{k,l=1}^2 J_{ckl} \sin(\phi_k^B - \phi_l^A), \quad (2)$$

where

$$\begin{aligned} J_{c11} &= (2e/m_a^* t) \tilde{n}_1^A \tilde{n}_1^B \\ J_{c21} &= (2e/m_\nu^* t) \tilde{n}_1^A \tilde{n}_2^B \\ J_{c12} &= (2e/m_\nu^* t) \tilde{n}_2^A \tilde{n}_1^B \\ J_{c22} &= (2e/m_b^* t) \tilde{n}_2^A \tilde{n}_2^B \end{aligned}, \quad (3)$$

$m_a^*, m_\nu^*, m_b^*$  are the effective masses that enter into the Ginzburg-Landau equations.

We restrict to the case where  $B$  is  $s$ -wave. In this case  $\tilde{n}_1^B = 0$ , and  $\tilde{n}_2^B = \text{constant}$ . We define  $\phi = \phi_2^B - \phi_1^A$ , as the relative phase difference between the two superconductors. We consider the case where the intrinsic phase difference within superconductor  $A$  is  $\phi_2^A - \phi_1^A = \pi/2$ . Then the supercurrent density can be written as:

$$J(\phi) = \tilde{J}_c \sin(\phi + \phi_c), \quad (4)$$

with

$$\tilde{J}_c = \sqrt{J_1^2 + J_2^2}, \quad (5)$$

$$\phi_c = \begin{cases} \tan^{-1} \frac{J_2}{J_1}, & J_1 > 0 \\ \pi + \tan^{-1} \frac{J_2}{J_1}, & J_1 < 0 \end{cases}, \quad (6)$$

where  $J_1 = J_{c21}$ ,  $J_2 = -J_{c22}$ . Two special cases are the following:

i) For  $d_{x^2-y^2} + is$  wave case  $\tilde{n}_1^A = n_{10} \cos(2\theta)$  is the magnitude of the  $d_{x^2-y^2}$ -wave component in (1),  $\theta$  is the angle of the crystalline  $a$ -axis of superconductor  $A$  with

the junction interface. The magnitude of the secondary order parameter is  $\tilde{n}_2^A = n_{20} = 0.1n_{10}$ .

ii) For  $d_{x^2-y^2} + id_{xy}$  wave case, the magnitude of the  $d_{x^2-y^2}$ -wave component in (1) is given by  $\tilde{n}_1^A = n_{10} \cos(2\theta)$ , while the  $d_{xy}$  wave component is  $\tilde{n}_2^A = n_{20} \sin(2\theta)$ . This order parameter can occur in the following way: The order parameter magnitude for the  $d$ -wave state is an equal admixture of pairs with orbital moment  $L_z = \pm 2$ ,  $\Delta_0(\Theta) = \Delta_0 \cos(2\Theta) = (\Delta_0/2)[\exp(2i\Theta) + \exp(-2i\Theta)]$ . In the presence of perturbation such as (ferromagnetically) ordered impurity spins  $S_z$  the coefficients of  $L_z = \pm 2$  components will shift linearly in  $S_z$  with opposite signs. The final state will be  $\Delta_0(\Theta) \rightarrow \Delta_0(\Theta) + iS_z\Delta_1(\Theta)$ , where  $\Delta_1(\Theta) = \sin(2\Theta)$ .

## III. THE JUNCTION GEOMETRY

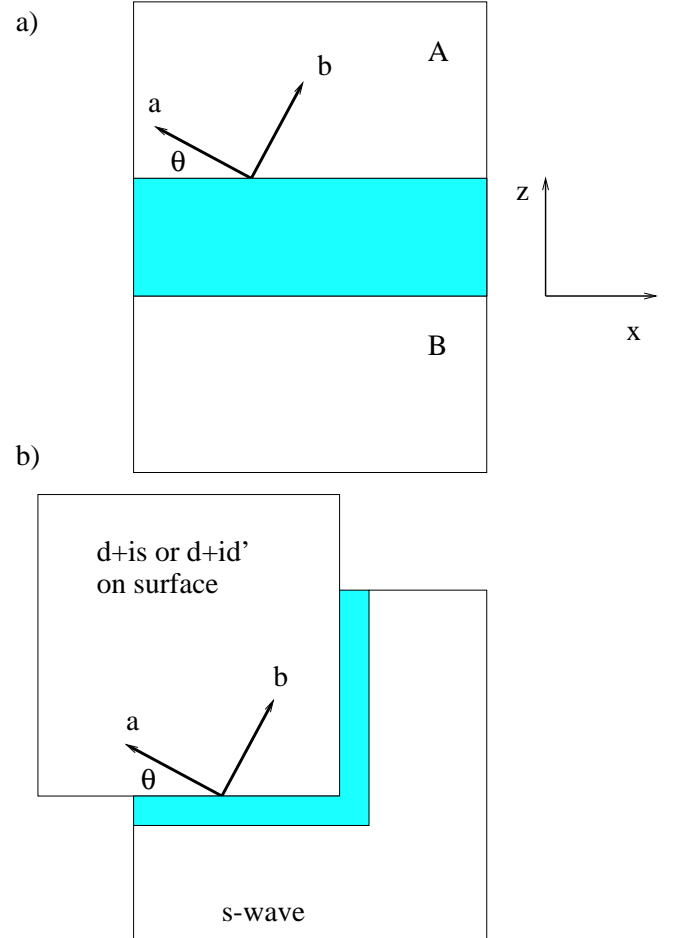


FIG. 1. (a) A single Josephson junction between superconductors  $A$  and  $B$  with a two component order parameter. The angle between the crystalline  $a$  axis of  $A$  and the junction interface is  $\theta$ . (b) The geometry of the corner junction between a mixed symmetry superconductor, and an  $s$ -wave superconductor.

We consider the corner junction shown in Fig. 1(b), between a superconductor with mixed wave symmetry at the surface and an s-wave superconductor. If the angle of  $a$ -axis with the interface in the  $x$ -direction is  $\theta$ , then the corresponding angle in the  $z$ -direction will be  $\pi/2 - \theta$ . We map the two segments of this junction into a one-dimensional axis. In this case the 2-D junction can be considered as being made of two 1-D junctions described above connected in parallel. Their characteristic phases  $\phi_{c1}$  and  $\phi_{c2}$  depend upon the angle  $\theta$ . The fabrication details of corner junctions or SQUIDS, between sample faces at different angles can be found in Ref. [2,10].

The superconducting phase difference  $\phi$  across the junction is then the solution of the sine-Gordon equation

$$\frac{d^2\phi(x)}{dx^2} = \frac{1}{\lambda_J^2} \sin[\phi(x) + \phi_c(x)] + I^{ov}, \quad (7)$$

where  $\phi_c(x) = \phi_{c1}(\phi_{c2})$  in the left (right) part of the junction. The relative phase  $\phi_c(x)$  and the critical current density  $\tilde{J}_c$  depends implicitly on the grain orientation.  $I^{ov}$  is the external current. The Josephson penetration depth is given by

$$\lambda_J = \sqrt{\frac{\hbar c^2}{8\pi e t \tilde{J}_c}},$$

where  $t$  is the sum of the penetration depths in two superconductors plus the thickness of the insulator layer.

We can classify the different solutions obtained from Eq. (7) with their magnetic flux content

$$\Phi = \frac{\Phi_0}{2\pi}(\phi_R - \phi_L), \quad (8)$$

where  $\phi_{R(L)}$  is the value of  $\phi$  at the right(left) edge of the junction, and  $\Phi_0 = \frac{\hbar c}{2e}$  is the flux quantum.

#### IV. SPONTANEOUS MAGNETIC FLUX AND CRITICAL CURRENTS

We will analyze the physics of the vortices, that exist in the frustrated junction geometry, discussed in Sec. III. These vortices are described by the variation of the phase  $\phi$ , along the junction. Regardless from the spatial variation of  $\phi$  in the interior, according to (8), the flux content of the vortex solutions is determined from the value of the phase  $\phi_{L(R)}$  at the left(right) edge of the junction, given, for zero current and external magnetic field, from the boundary conditions

$$d\phi/dx|_{x=0,L} = 0 = \sin[\phi_{L(R)} + \phi_c(x)], \quad (9)$$

where  $\phi_{L(R)}$  is the phase at  $x = 0$  and  $x = L$  respectively, and it crucially depends on the values of  $\phi_{c1}$  and  $\phi_{c2}$ .

If we restrict to the case where  $\phi_{c1} \approx 0$  and  $\phi_{c2} \approx -\pi$ , some special values for  $\phi_{L(R)}$  are:

One case would be that in which  $\phi_{L(R)} = -\phi_{c1}(-\phi_{c2})$ . We label this solution as  $f_{va}$ .

At the same time another solution of the (9) is  $\phi_L = -\phi_{c1}$ , and  $\phi_R = -2\pi - \phi_{c2}$ . This solution is labeled as  $f_a$ , because it corresponds to negative flux. We expect and this is verified later from the numerical simulations that the phase varies smoothly from  $-\phi_{c1}$  to  $-2\pi - \phi_{c2}$  as  $x$  goes from one edge of the junction to the other. Note that although the value of the phase at  $x = L$  is  $-\phi_{c2}$  boosted by  $2\pi$  the magnetic flux in the junction is  $(-2\pi - \phi_{c2} + \phi_{c1})/2\pi$ , which is quite different from the corresponding value for the  $f_{va}$  solution. The flux content for the latter case is  $(-\phi_{c2} + \phi_{c1})/2\pi$ . So we expect and this is verified later by the numerical calculation of the critical current and the enclosed flux, that both the above solutions for the phase  $\phi$  correspond to physical quantities with different properties.

With the same way of thinking there is another solution of (9), which is  $\phi_L = -2\pi - \phi_{c1}$ , and  $\phi_R = -\phi_{c2}$ . The enclosed flux corresponding to this solution  $(-\phi_{c2} + \phi_{c1} + 2\pi)/2\pi$  is positive over the range of variation of  $\theta$ . We call this solution as fractional vortex  $f_v$ .

The above results can be verified from a more general point of view. Following Sigrist [16] we discuss the formation of vortices in a junction with time reversal symmetry breaking, where the internal phase difference  $\phi_c(x)$  is given by (6), and we restrict to the interval  $-\pi, \pi$ , for the values of arctan. For  $0 < x < L/2$  the stable solutions for the s-G equation is  $\phi(x) = -\phi_{c1} + 2n_1\pi$ , where  $n_1 = 0, \pm 1, \pm 2, \dots$ , while for  $L/2 < x < L$  the stable solutions for the s-G equation is  $\phi(x) = -\phi_{c2} + 2n_2\pi$ , where  $n_2 = 0, \pm 1, \pm 2, \dots$ . When the frustrated junction is formed, and we consider the above junctions in parallel, the phase  $\phi$  is forced to change around  $x = L/2$ , to connect these stable solutions. The resulting phase  $\phi$  encloses flux in units of  $\Phi_0$

$$\Phi = [\phi(L) - \phi(0)]/2\pi = (-\phi_{c2} + \phi_{c1} + 2n\pi)/2\pi, \quad (10)$$

where  $n = n_1 - n_2 = 0, \pm 1, \pm 2, \dots$  In particular

$$\begin{aligned} n = 0 \quad \Phi &= (-\phi_{c2} + \phi_{c1})/2\pi & f_{va} \\ n = 1 \quad \Phi &= (-\phi_{c2} + \phi_{c1} + 2\pi)/2\pi & f_v \\ n = -1 \quad \Phi &= (-\phi_{c2} + \phi_{c1} - 2\pi)/2\pi & f_a \end{aligned}, \quad (11)$$

So the analysis above is an application of (10), or relation 6.5 of Ref. [16], for the particular values  $n = 0, 1, -1$ , corresponding to the  $f_{va}, f_v, f_a$  respectively. Generally the flux content is fractional i.e. is neither integer nor half-integer, as a consequence of the broken time reversal symmetry of the problem.

In the case of  $0 - \pi$  junction, where the internal phase in the right (left) part of the junction is  $\phi_{c2} = -\pi$  ( $\phi_{c1} = 0$ ), the stable solutions of the s-G equation are  $\phi(x) = 2n\pi$  for the left part, while  $\phi(x) = \pi(2n+1)$  for the right part of the junction. In this case a  $0 - \pi$  junction is formed. The corresponding flux becomes  $\Phi = (\pi + 2n\pi)/2\pi$ , and

the particular values of  $n = 0, n = 1$  give the half vortex and antivortex solutions, with opposite fluxon content,  $\Phi = 0.5$  and  $\Phi = -0.5$  respectively.

For the  $0 - 0$  junction  $\phi_{c1} = \phi_{c2} = 0$ , and the flux becomes  $\Phi = n$ , so we say that the flux is quantized in integer units of  $\Phi_0$ . In this case, there exist solutions with flux  $\Phi = \dots, -1, 0, 1, \dots$ . These solutions, when  $n \neq 0$  are stabilized by the application of an external magnetic field. Here, the external field is not necessary due to the spontaneous magnetization.

In the actual numerical simulations, for example for the  $f_{va}$  solution the phase  $\phi(x)$  is taken  $\phi(x) = -\phi_{c1}$  ( $-\phi_{c2}$ ) in the left (right) part of the junction, as an initial condition and then is iterated until convergence. Besides if we take as initial condition,  $-\phi_{c1}$ , in the left side, and  $\phi = -2\pi - \phi_{c2}$  in the right side, the final state of the system, after the iteration procedure, is the solution which we call  $f_a$ , with negative magnetic flux, and not exactly opposite to  $f_{va}$ . We comment here that the solutions after the iteration procedure have smooth variation as a function of the position, as opposed to the step function variation of the initial conditions.

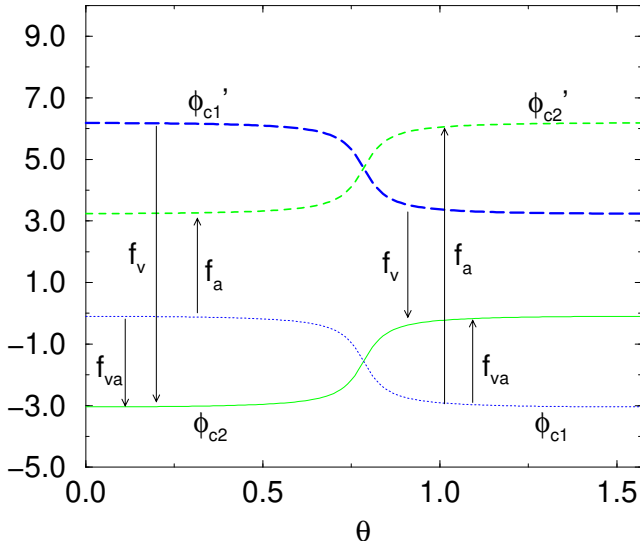


FIG. 2. The variation of  $\phi_{c1}, \phi_{c2}$  with the angle  $\theta$ . For each value of  $\theta$  there exist three vortex solutions which are depicted by arrows. Up(down) arrow denotes negative(positive) flux.

For the  $d_{x^2-y^2} + is$ -wave case, we consider first the situation where  $\theta$  is varied from 0 to  $\pi/2$ . We plot in Fig 2. the variation of  $\phi_{c1}$  and  $\phi_{c2}$  with the angle  $\theta$ , as obtained from (6), where the values of arctan is strictly in the interval  $[-\pi, \pi]$ . As a guide for the eye we also plot  $\phi'_{c2} = 2\pi + \phi_{c2}$  and  $\phi'_{c1} = 2\pi + \phi_{c1}$ , as a function of  $\theta$ . For each value of  $\theta$  there exist three kinds of solitons which are depicted in Fig. 2 by arrows. Up (down) arrow denotes negative (positive) flux. As discussed earlier the arrows correspond to the variation of the phase from the left to the right part of the junction.

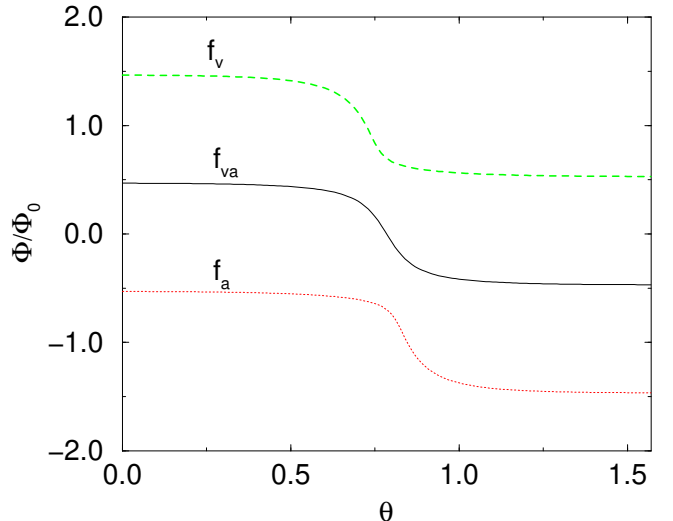


FIG. 3. The spontaneous magnetic flux  $\Phi$  as a function of the angle  $\theta$ , for the  $f_v, f_{va}, f_a$  solutions, for a  $d_{x^2-y^2} + is$  junction with length  $L = 10\lambda_J$ .

In Fig. 3 we plot the magnetic flux at zero current versus the angle ( $\theta$ ) for the different solutions described above. We see a characteristic variation with the orientation through  $\theta = \pi/4$ , for the  $f_{va}$  solution. At this point the magnetic flux is zero. The other two patterns  $f_v, f_a$ , are shifted in opposite direction from  $\pi/4$ .

The argument that all the above solutions correspond to physical quantities is further supported from the eigenvalue analysis and the calculation of the energy of the spontaneous solutions as a function of angle  $\theta$ . The corresponding equations can be found in Ref. [11]. We see from Fig. 4. (up) that, the  $f_{va}$  solution has the lowest energy. However, for angles close to  $\theta = 0$  ( $\pi/2$ ) the energy for the  $f_a$  ( $f_v$ ) is quite close to that of the  $f_{va}$ . From the stability analysis, presented in Fig. 4 (down), we see that, the  $f_{va}$  solution appears to be stable over the whole range of  $\theta$  variation, while  $f_a$  is stable only for  $\theta < \pi/2$ . We believe that since these two solutions are stable for  $I = 0$ , they will both lead to observable critical currents when increasing the bias current, for these angles  $\theta$ . This is not true for the  $f_v$  solution which in the same angle values has flux greater than  $\Phi_0$  and is unstable as seen in Fig. 4. This solution can be stabilized by an external magnetic field. We conclude that only the region in  $\theta$  with magnetic flux smaller than  $\Phi_0$  corresponds to stable solutions.

In Fig. 5 we plot the overlap critical current  $I_c^{ov}$  as a function of  $\theta$ , for  $H = 0$ , for the  $f_v, f_{va}, f_a$  solutions. Note the overlapping between different branches. We see a reduction at  $\theta = \pi/4$  caused by the small value of  $\tilde{J}_c$  at this angle. It seems that increasing  $I_c^{ov}$  does not change the flux.

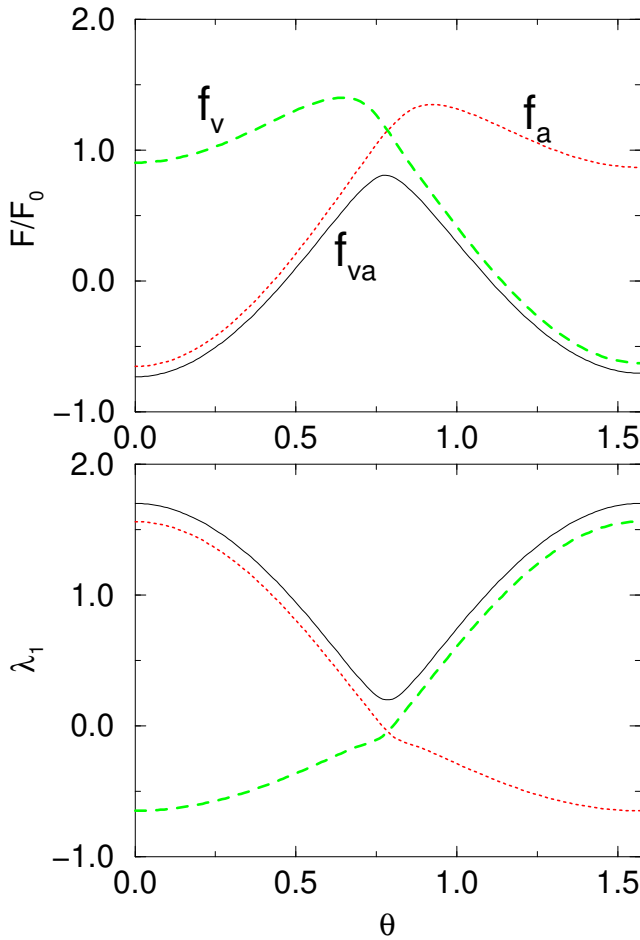


FIG. 4. Energy of the spontaneous solutions  $F/F_0$  (up), and the lowest eigenvalue  $\lambda_1$  (down) as a function of angle  $\theta$ , for the  $f_{va}$ ,  $f_a$ ,  $f_v$  solutions. In the range where  $\theta$  is close to zero, both  $f_{va}$ , and  $f_a$  correspond to stable solutions.

In the following we study separately the critical current, and flux content for different orientations:

a)  $\theta = 0$

For the  $f_{va}$  solution, at  $I^{ov} = 0$ , the phase goes from  $-\phi_{c1} \approx 0$  to  $-\phi_{c2} \approx \pi$  as seen in Fig. 6a, where we have plotted the phase distribution for the  $f_{va}$ ,  $f_a$ ,  $f_v$  solutions, at  $\theta = 0$ . Increasing  $I^{ov}$  simply displays this solution around  $\phi = \pi$ . For the  $f_a$  solution, the phase goes from  $-\phi_{c1}$  to  $-2\pi - \phi_{c2}$ , at  $I^{ov} = 0$ . The current distribution at  $I_c^{ov}$  has a small reduction around  $x = L/2$  and if we take into account the  $\tilde{J}_c > 1$  at this point increases the  $I_c^{ov} > 1$ .

b)  $\theta = \pi/4$

For the  $f_{va}$ , the point  $I^{ov} = 0$  corresponds to a flat phase distribution around  $\pi/2$ ,  $\phi_{c1} \approx \phi_{c2} \approx -\pi/2$ , as seen in Fig. 6b. Increasing  $I^{ov}$  displays the distribution close to  $\pi$  and the current distribution is maximum ( $\approx 1$ ), but the almost zero value of the  $\tilde{J}_c$  reduces the critical current density to a minimum at this point. For the  $f_a$ , at  $\theta = \theta'$  where  $\theta'$  is less but close to  $\pi/4$ , a full antifluxon enters the junction.

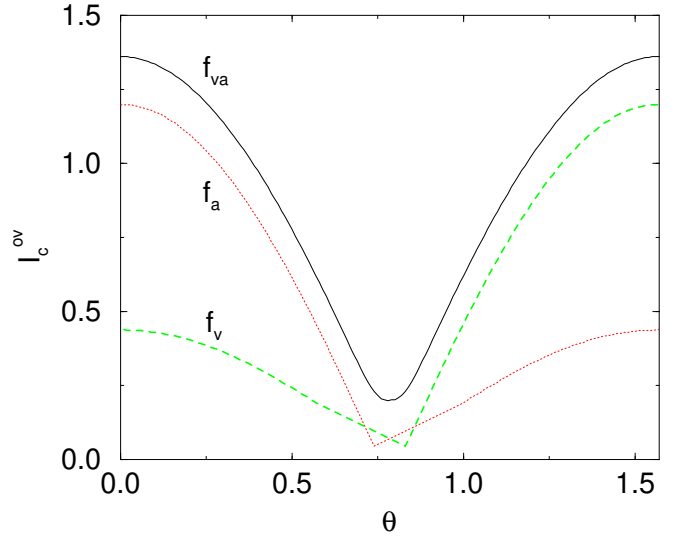


FIG. 5. Critical current  $I_c^{ov}$  versus the angle  $\theta$  for a junction with  $d_{x^2-y^2} + is$  symmetry, and length  $L = 10\lambda_J$ . The branches for the different vortex solutions overlap with each other.

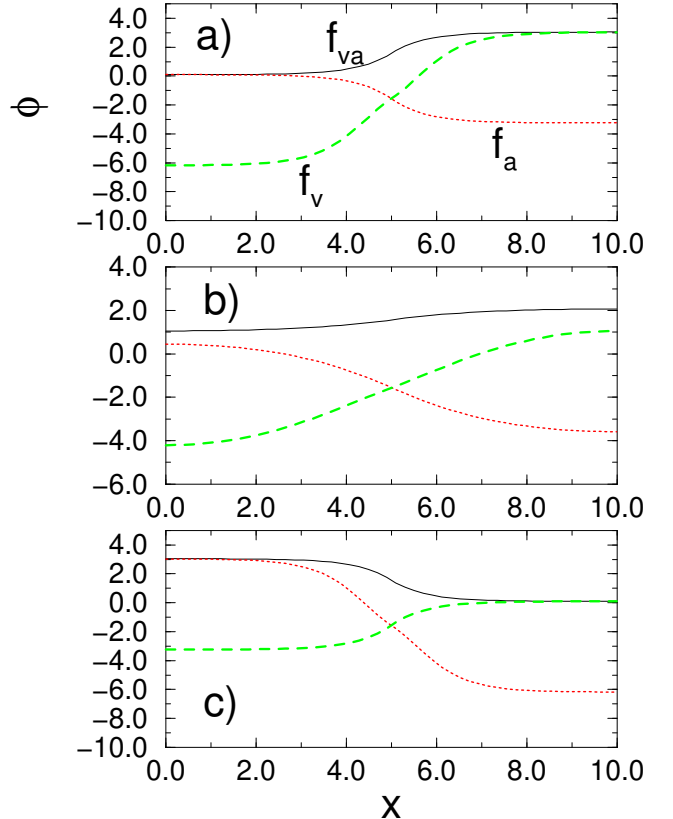


FIG. 6. The phase distribution of the vortex solutions  $f_{va}$ ,  $f_a$ , and  $f_v$ , at a)  $\theta = 0$ , b)  $\theta = \pi/4$ ,  $\theta = \pi/2$ , for a junction with  $d_{x^2-y^2} + is$  symmetry, length  $L = 10\lambda_J$ , and zero external current  $I^{ov} = 0$ .

The corresponding current distribution is symmetric

around zero leading to an almost zero critical current at this point.

c)  $\theta = \pi/2$

At this orientation, the  $f_{va}$  solution, as we can see from Fig. 2, the constants  $\phi_{c1}$  and  $\phi_{c2}$  take the values,  $\phi_{c1} \approx -\pi$ ,  $\phi_{c2} \approx 0$ . The phase goes from  $-\phi_{c1} \approx \pi$  to  $-\phi_{c2} \approx 0$ . The critical current is the same as in  $\theta = 0$ . For the  $f_a$ , at  $\theta = \pi/2$ ,  $I_c^{ov} = 0$ , the phase goes from  $\approx \pi$  to  $\approx -2\pi$ . At the critical current the asymmetric current distribution decreases  $I_c^{ov}$  to the value we see in Fig. 5.

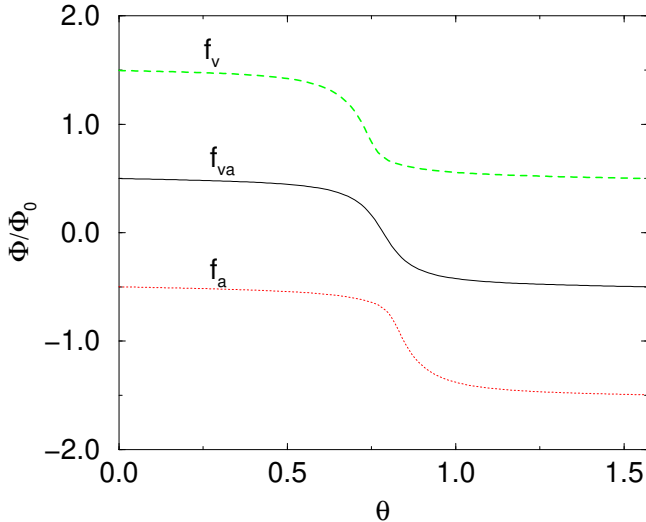


FIG. 7. The spontaneous magnetic flux  $\Phi$  as a function of the angle  $\theta$ , for the  $f_v$ ,  $f_{va}$ ,  $f_a$  solutions, for the  $d_{x^2-y^2} + id_{xy}$ -wave pairing state.

For the  $d_{x^2-y^2} + id_{xy}$  pairing symmetry state, we plot in Fig. 7 the flux content for the  $f_v$ ,  $f_{va}$ ,  $f_a$ , versus the angle  $\theta$ . The main difference with the  $d_{x^2-y^2} + is$  state is the integer or half integer value of  $\Phi$  at  $\theta$  close to 0 or  $\pi/2$ , compared to the fractional value for the  $d_{x^2-y^2} + is$  case. This happens because the imaginary  $d_{xy}$  component vanishes for this grain orientation, leading to pure  $d$ -wave order parameter at this angle.

In Fig. 8 we plot the critical current evolution with the grain angle  $\theta$ . Close to  $\theta = 0$  we see that the  $I_c^{ov}$  for the  $f_{va}$ ,  $f_a$  solutions, coincide. This happens also at  $\theta = \pi/2$  for the  $f_{va}$ ,  $f_v$  solutions. The critical current at these angles is the same as in a junction with pure  $d$ -wave symmetry, for the reason we mention before. Also we see that for  $\theta = \pi/4$ , the critical currents for both junctions coincide due to the same magnitude of the order parameter at this angle i.e., for  $\theta = \pi/4$ ,  $\sin[2(\pi/4)] = 1$ . Also the unstable part of the  $f_v$  branch, in the  $I_c$  vs  $\theta$  is almost the same for the two symmetry states, due to the small difference in the flux, compared with the large flux content of the solutions in this region.

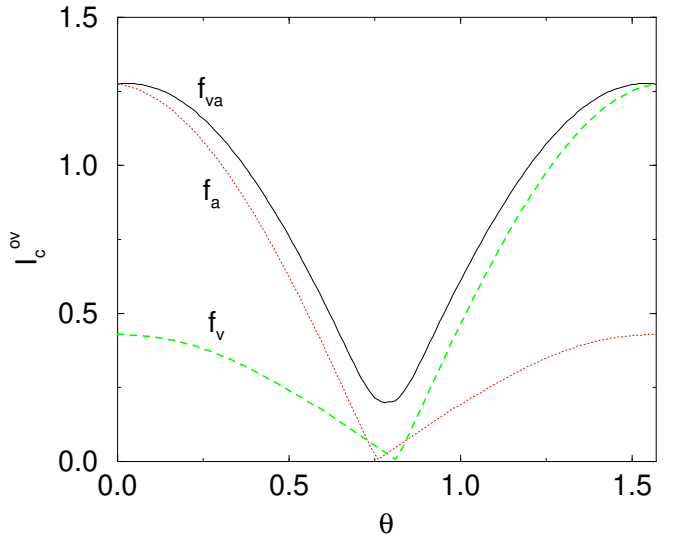


FIG. 8. Critical current  $I_c$  versus the angle  $\theta$  for a junction with  $d_{x^2-y^2} + id_{xy}$  symmetry, and length  $L = 10\lambda_J$ . The branches for the different vortex solutions overlap with each other.

## V. MAGNETIC FIELD EFFECTS

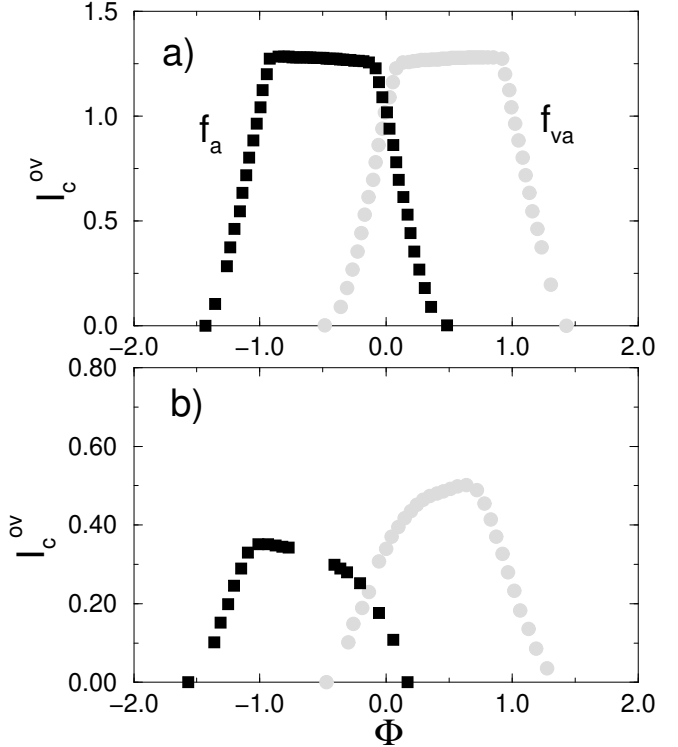


FIG. 9. (a) Overlap critical current  $I_c^{ov}$  versus the magnetic flux  $\Phi$  in units of  $\Phi_0$ , for a junction with  $d_{x^2-y^2} + id_{xy}$  symmetry, length  $L = 10\lambda_J$ , for angle  $\theta = 0^\circ$ . (b) The same as in a) but for  $\theta = 0.63$ . Only the stable solutions  $f_{va}$ ,  $f_a$ , are presented.

We now examine the magnetic-interference pattern for the two symmetries. In the  $d_{x^2-y^2} + id_{xy}$ -wave case, where  $\theta = 0$ , this pattern has a symmetric form as we can see from Fig. 9(a). This is due to the  $d_{x^2-y^2}$ -wave like form of the order parameter at this angle. Note that only the stable solutions in this range of  $\theta$  angles  $f_{va}$ ,  $f_a$ , appear in the plot. For the angle  $\theta = 0.63$  this pattern becomes asymmetric and the "dip" appears to a value of flux different than zero. Also the critical current is much reduced compared to the case where  $\theta = 0$  as can be seen in Fig. 9(b).

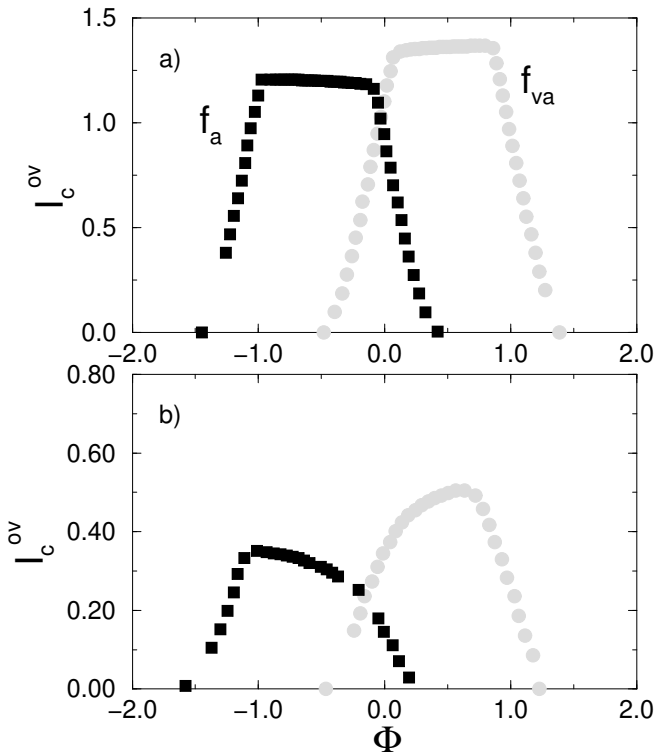


FIG. 10. Overlap critical current  $I_c^{ov}$  versus the magnetic flux  $\Phi$  in units of  $\Phi_0$ , for  $f_{va}$ ,  $f_a$  solutions, for a junction with  $d_{x^2-y^2} + is$  symmetry, and length  $L = 10\lambda_J$ , for angle  $\theta = 0^\circ$ . (b) The same as in a) but for  $\theta = 0.63$ . Only the stable solutions  $f_{va}$ ,  $f_a$ , are presented.

In the  $d_{x^2-y^2} + is$  symmetry, in the limit where  $\theta \rightarrow 0$ , the pattern is asymmetric for the  $d_{x^2-y^2} + is$  case, as can be seen in Fig. 10a, for the angle  $\theta = 0$ . This is in agreement with our previous work for the inline current dependence of the magnetic field for a junction with  $d_{x^2-y^2} + is$  symmetry [11]. There it was found that the pattern is asymmetric for lengths as long as  $L = 10\lambda_J$ . For angles close to  $\pi/4$ , the magnetic interference pattern is similar with the  $d_{x^2-y^2} + id_{xy}$ -state. This is because the  $\sin(2\theta)$  dependence of the  $d_{xy}$  component is almost unity. This is seen in Fig. 10b where we present the variation of the critical current versus the enclosed flux for  $\theta = 0.63$ , and the symmetry state is  $d_{x^2-y^2} + is$ .

So in the limit where  $\theta \rightarrow 0$ , the magnetic interfer-

ence pattern is symmetric(asymmetric) for the  $d_{x^2-y^2} + id_{xy}$ ( $d_{x^2-y^2} + is$ ) and this can be used to distinguish between these two symmetry states. We argue here that an other measurement is needed at an angle  $\theta$  close to  $\pi/4$  where both patterns are asymmetric, to exclude the pure  $d_{x^2-y^2}$ -wave case, which appears to be symmetric everywhere.

## VI. CONCLUSIONS

We have studied the static properties of a one-dimensional junction with  $d_{x^2-y^2} + is$  or  $d_{x^2-y^2} + id_{xy}$  order parameter symmetry. The variation of the critical current  $I_c^{ov}$  with grain orientation can give us information about the pairing symmetry, at least where junctions are formed.

We have followed the evolution of spontaneously formed vortex and antivortex solutions for different angle of the crystalline  $a$ -axis and the junction interface. We have shown that for some range of  $\theta$  where the magnetic flux content is greater than unity, the vortex solution becomes unstable. We conclude that when a mixing state symmetry is realized, the evolution of the fractional vortex and antivortex solutions is different for the two symmetry states we propose and this may distinguish one from the other.

We expect our findings, for the magnetic field dependence of the critical current, to hold even in the short junction limit, where the most experiments on corner junctions have been performed [2,10].

---

- [1] D.J. Scalapino, Phys. Rep. **250**, 329 (1995).
- [2] D.J. van Harlingen, Rev. Mod. Phys. **67**, 515 (1995).
- [3] J.R. Kirtley, P. Chaudhari, M.B. Ketchen, N. Khare, S.Y. Lin, and T. Shaw, Phys. Rev. B **51**, 12 057 (1995).
- [4] A.V. Balatsky, Phys. Rev. Lett. **80**, 1972 (1998).
- [5] A.V. Balatsky, Phys. Rev. B **61**, 6940 (2000).
- [6] M. Covington, M. Aprili, E. Paraoanu, L.H. Green, F. Xu, J. Zhu, and C.A. Mirkin, Phys. Rev. Lett. **79**, 277 (1997).
- [7] M. Fogelstrom, D. Rainer, and J.A. Sauls, Phys. Rev. Lett. **79**, 281 (1997).
- [8] M. Aprili, E. Badica, and L.H. Greene, Phys. Rev. Lett. **83**, 4630 (1999).
- [9] R. Krupke, and G. Deutscher, Phys. Rev. Lett. **83**, 4634 (1999).
- [10] D.J. van Harlingen, J.E. Hilliard, B.L.T. Plourde and B.D. Yanoff, Physica C **317-318**, 410 (1999).
- [11] N. Stefanakis, and N. Flytzanis, Phys. Rev. B **61**, 4270 (2000).
- [12] T. Kato, and M. Imada, J. Phys. Soc. Jpn. **65**, 2963 (1996).

- [13] D.B. Bailey, M. Sigrist, and R.B. Laughlin, Phys. Rev. B **55**, 15 239 (1997).
- [14] L.G. Aslamazov and A.I. Larkin, Pis'ma Zh. Eksp. Teor. Fiz. **9**, 150 (1968) [JETP Lett. **9**, 87 (1969)].
- [15] J.-X. Zhu, W. Kim, and C.S. Ting, Phys. Rev. B **58**, 6455 (1998).
- [16] M. Sigrist, Prog. Theor. Phys. **99**, 899 (1998).